DOI: 10.26599/FSHW.2025.9250655

Contents lists available at SciOpen

Food Science and Human Wellness

journal homepage: https://www.sciopen.com/journal/2097-0765

China Food Publishing Co.

Uncovering the detoxifying power of *Glycyrrhizae* Radix et Rhizoma: A Breakthrough in Combating Psoraleae Fructus-Induced Liver Injury by suppressing NLRP3 inflammasome activation

Yingjie Xu[a,b,c#], Longxin Guo[b,c,d#], Jincai Wen[b,c#], Wen Kan[b,c], Caiping He[b,c], Zhanjiang Hu[b,c,d], Ping Zhang[e], Yuming Guo[f], Xiaoyan Zhan[b,c,g*], Xiaohe Xiao[a,b,c,d,g*], Zhaofang Bai[b,c,d,g*]

[a] *School of Pharmacy, Nanjing University of Chinese Medicine, Nanjing, 210023, China*

[b] *Senior Department of Hepatology, The Fifth Medical Center of PLA General Hospital, Beijing, 100039, China*

[c] *China Military Institute of Chinese Materia, The Fifth Medical Centre, Chinese PLA General Hospital, Beijing, 100039, China*

[d] *School of Pharmacy, Dali University, Dali, 671000, China*

[e] *Department of Pharmacy, Medical Supplies Center of PLA General Hospital, Beijing 100039, China.*

[f] *Department of Infectious Diseases, The Fifth Medical Center of Chinese PLA General Hospital, National Clinical Research Center for Infectious Diseases, Beijing, 100039, China*

[g] *National Key Laboratory of Kidney Diseases, Beijing, 100039, China*

ABSTRACT: Drug-induced liver injury (DILI) is an adverse drug reaction that results in acute liver failure or even death in severe cases. Recently, the incidence of DILI caused by Psoraleae Fructus (PF), a widely used tonic in clinical medicine, has increased. However, no effective method for mitigating hepatotoxicity has been identified. *Glycyrrhizae* Radix et Rhizoma (GR) is a functional food with known detoxifying and hepatoprotective properties. Therefore, this study aimed to investigate the potential effect of GR in mitigating PF-induced hepatotoxicity and to elucidate the underlying mechanisms. A rat model of lipopolysaccharide (LPS)-induced immune stress was established to examine the ameliorative effect of GR on PF-induced hepatotoxicity. GR reduced PF-induced increase in the levels of liver injury markers, downregulated the levels of inflammatory factors and oxidative stress, and ameliorated pathological changes in liver tissue. Pathway analysis of 37 differentially expressed metabolites following GR treatment showed that the metabolites were mainly enriched in pathways associated with the NOD-like receptor pyrin domain-containing protein 3 (NLRP3) inflammasome. In vitro, GR effectively inhibited PF-induced NLRP3 inflammasome activation in LPS-stimulated bone marrow-derived macrophages (BMDMs), providing a novel therapeutic strategy for managing PF-induced hepatotoxicity and guidance for the rational clinical use of PF.

Keywords: Drug-induced liver injury; Psoraleae Fructus; *Glycyrrhizae* Radix et Rhizoma; NLRP3 inflammasome; Metabolomics

1. Introduction

Drug-induced liver injury (DILI), caused by drugs or their metabolites, is a serious global clinical problem. In the United States, over 50% of reported acute liver failure cases are attributed to DILI[1, 2].

[#]These authors have contributed equally to this work.
***Corresponding author**
baizf2008@hotmail.com; pharmacy_302@126.com

Received 26 December 2024
Received in revised from 30 January 2025
Accepted 16 April 2025

Although traditional Chinese medicines (TCM) are generally regarded as "safe," recent studies have implicated some TCM in DILI, causing global public concern[3]. Cases of liver injury associated with Psoraleae Fructus (PF)-containing preparations have been documented in China, South Korea, Germany, and India[4, 5]. Furthermore, the National Center for Adverse Drug Reactions (NCAR) has reported liver injury associated with PF-containing preparations, including Zhuang gu guan jie pills (ZGW) and Xian ling gu bao capsules (XLGB). PF, derived from the dried fruit of *Psoralea corylifolia* L., is used to treat conditions such as kidney deficiency, impotence, lumbago, cold pain, and osteoporosis, and is a tonic medicine commonly used in Chinese medicine clinics[6, 7]. The mechanisms underlying PF-induced liver injury, including bile acid metabolism, oxidative stress, mitochondrial dysfunction, and suppression of hepatocyte regeneration, have been extensively investigated[8, 9]. In a previous study, we showed that PF and its components Psoralidin, Bakuchiol, and Bavachinin cause DILI, possibly by affecting immune inflammatory response[7, 10-12]. However, research on herbs that can attenuate the toxic effects of PF and their potential mechanisms remain scarce.

Glycyrrhizae Radix et Rhizoma (GR) is a functional food used as a sweetener and antioxidant. GR is used as an additive in toothpaste, cosmetics, and other products[13]. Additionally, its constituents are widely used in clinical practice because of their multifaceted pharmacological properties, including antitumor, anti-inflammatory, antiviral, and hepatoprotective properties[14]. GR is recognized as a functional food because of its detoxifying power, and is frequently used in the formulation of detoxifying herbs[15, 16]. Notably, the detoxification pathways of GR primarily involve anti-inflammatory actions, enhancement of toxic substance metabolism, and upregulation of p-glycoprotein expression and function. A previous study using a neurotoxicity rat model showed that GR mitigated the neurotoxic effects of Semen Strychni through the HMGB1-associated pathway[17]. Additionally, co-administration of GR and common Threewingnut root alleviated *Tripterygium wilfordii* toxicity by reducing epoxy diterpene ester compounds[18]. Previous studies have shown that licorice extract can ameliorate Methionine-Choline Deficient (MCD)-induced non-alcoholic fatty liver disease and improve inflammation in the liver by regulating the cGAS-STING pathway[19]. Moreover, the active ingredients in licorice, Licochalcone B[20] and Echinatin[21], are effective in decreasing the release of inflammatory factors (TNF-α, IL-6, and IL-1β) by affecting NOD-like receptor pyrin domain-containing protein 3 (NLRP3) inflammasome activation, thereby ameliorating liver inflammation. Glycyrrhizic acid preparations, such as diammonium glycyrrhizinate[22], have been used to treat chronic hepatitis and have important clinical applications in hepatic fibrosis and liver injury. Although the hepatoprotective effect of GR has been demonstrated, it is unclear whether it mitigates PF-induced hepatotoxic effects.

The inflammasome, an intracellular multi-protein complex predominantly found in innate immune cells, responds to external pathogens or endogenous danger signals to initiate inflammatory response[23, 24]. A diverse array of pathogen-associated molecular patterns, including bacteria, viruses, metabolites, and damage-associated molecular patterns, activate inflammasomes, which consist of sensing proteins (NLRP3,

AIM2, and NLRP1), adaptor proteins (ASC), and effector proteins (caspase-1)[25, 26]. NLRP3 inflammasome has been extensively studied for its role in innate immunity and inflammation. NLRP3 inflammasome activation triggers caspase-1-mediated cleavage of the precursor cytokines pro-IL-1β and pro-IL-18, resulting in the liberation of the mature cytokines IL-1β and IL-18[27, 28]. Aberrant inflammasome activation has been linked to several diseases, including DILI, autoimmune diseases, and metabolic disorders[29, 30]. Further research has indicated that targeting inflammasomes is a potential therapeutic strategy for various diseases[31, 32]. For example, Licorice chalcone B (LicoB) and Echinatin can mitigate DILI by inhibiting inflammasome activation[20, 21], suggesting that targeting NLRP3 inflammasomes may be a promising approach to ameliorate DILI.

In this study, we investigated the potential of GR to mitigate PF-induced hepatotoxicity and explored the underlying mechanisms using a rat model of lipopolysaccharide (LPS)-induced immune stress. Metabolomic analysis was performed to explore the mechanisms underlying PF-induced changes in rat. Additionally, we established an inflammasome activation model in bone marrow-derived macrophages (BMDMs) for validation, providing a theoretical foundation for the safe clinical application of PF.

2. Experimental Section

2.1 Analysis of constituents within the alcoholic extracts of PF and GR

The medicinal materials were crushed, extracted twice with 75% ethanol, concentrated to a certain volume with a vacuum rotary evaporator, and dried for more than 12 h to obtain the PF and GR alcohol extracts. Both the PF and GR extracts were prepared by dissolving and diluting in a 20% methanol solution, ensuring thorough mixing and subsequent filtration. Thereafter, the constituents of the prepared samples were analyzed using a Waters UPLC system coupled with UltimateXB-C18 column (4.6 mm × 150 mm; 3 μm). Acetonitrile served as mobile phase A, and 0.1% (v/v) phosphoric acid solution was used as mobile phase B. Detection of PF compounds was performed at 246 nm, and GR compounds were detected at 236 nm for 0–50 min and 375 nm for 50–56 min. Finally, the resulting chromatograms were compared with the PF and GR reference profiles to determine their compositions.

2.2 Mice

Male Sprague-Dawley (SD) weighing 250–300 g (n = 48; 7–8-week-old) were procured from Beijing SPF Biotechnology Co., Ltd., and housed in the Laboratory Animal Center of the Fifth Medical Center at the General Hospital of the Chinese People's Liberation Army. All animal experiments were approved by the Fifth Medical Center at the General Hospital of the Chinese People's Liberation Army (ethical approval no.: IACUC-2023-0008). During the study, the rats were housed in a specific-pathogen-free environment under controlled conditions (room temperature, 22 ± 2 °C; relative humidity, 45–55%).

2.3 LPS-induced immune stress model

After a 7-day acclimation period, the rats were divided into six groups based on body weight (n = 8 rats/group): control, LPS, PF, LPS + GR, LPS + PF (LP), and LPS + PF + GR (LPG). After 3 days of GR

administration via gavage, PF and GR were administered simultaneously to rats in the LPG group at a dose of 3.6 g/kg each, according to the literature[7]. After 3 h, LPS was injected into the tail vein of rats in the LPS, LPS + GR, LPS + PF (LP), and LPS + PF + GR (LPG) groups. In contrast, rats in the control and PF groups received equivalent volumes of saline solution. After 8 h, the rats were anesthetized using 1% sodium pentobarbital injection, followed by the collection of venous blood and hepatic tissues. Serum concentrations of alanine aminotransferase (ALT) and aspartate aminotransferase (AST) were measured. Serum IL-1β and IL-18 levels were determined using relevant enzyme-linked immunosorbent assay (ELISA) kits. Additionally, serum malondialdehyde (MDA) levels and superoxide dismutase (SOD) and glutathione (GSH) activities were determined. Histological analysis of hepatic samples was performed using hematoxylin and eosin (H&E) staining. Moreover, the mRNA levels of IL-1β, IL-18, NLRP3, and caspase-1 in the hepatic tissue were determined using quantitative polymerase chain reaction (qPCR).

2.4 Liver histological observation

Hepatic tissues were fixed in 4% paraformaldehyde solution, dehydrated, embedded in paraffin, and cut into sections. Therefore, the tissue sections were stained with H&E, according to the manufacturer's instruction. Finally, pathological changes in the tissue sections were assessed using a microscope.

2.5 Reagents

PF and GR extracts were procured from Shanghai Winherb Medical Technology Co., Ltd. Fetal bovine serum (FBS; F101-01) was obtained from Vazyme (Nanjing, China). Mouse colony-stimulating factor (MCSF; HY-P7085), MCC950 (HY-12815A), and Nigerian (HY-12815A) were obtained from MedChemExpress (MCE, USA). ATP (A2383) was acquired from MilliporeSigma. DMEM (PYG0073) and mouse IL-18 antibody (EK0433) were provided by BOSTER in Wu Han, China. Caspase-1 antibody (1:1000, AG-20B-0042-C100) and NLRP3 antibody (1:1000, AG-20B-0014-C100) were purchased from Adipogen (San Diego, CA, USA). LaminB antibody (1:3000, 66095-1-Ig) was provided by Proteintech (USA). Mouse IL-1β (1210122) and rat IL-1β (1310122) ELISA kits were provided by Dakewe. ALT (c009-2-1) and AST (c010-2-1) kits were supplied by Jiancheng Biological Technology Co., Ltd., Nanjing, China. CytoTox 96 non-radioactive cytotoxicity assay kit (G1780) was provided by Promega. Rat IL-18 antibody (EK318) was purchased from Multisciences (Lianke) Biotech, Co., Ltd. StarScript III All-in-one RT Mix with gDNA Remover (A230-10), 2×RealStar Fast SYBR qPCR Mix (Low ROX) (A304-10), and StarRuler Color Prestrained Protein Marker (10-180 kDa) were purchased from GenStar (China). Echinatin (34221-41-5) is purchased from TagerMol (China).

2.6 Metabolomic profile

2.6.1 Metabolite extractions

Serum samples from the four distinct experimental groups, control (CON), LPS, LPS + PF (LP), and LPS + PF + GR (LPG), were collected in 50 μL Eppendorf tubes containing equal parts of methanol and acetonitrile. Thereafter, the mixture was agitated, ultrasonicated in a cold water-ice bath for 10 min, and stored

at -40 °C for 60 min. After centrifuging at 12,000 *g* for 15 min at 4 °C, the supernatant was carefully transferred to a sample-introduction device for subsequent analysis. Portions of the supernatant from each group were amalgamated to create a pooled quality control (QC) sample, which was also analyzed. QC samples were used to monitor the instrument stability and data quality to ensure the reliability of the data.

2.6.2 LC-MS analysis

The compositions of GR and PF were determined utilizing an Orbitrap Exploris 120 mass spectrometer coupled with a Waters ACQUITY UPLC BEH Amide column (2.1 mm × 50 mm; 1.7 μm) for liquid chromatographic separation. The temperature of the column was kept at 4 °C, and the volume of the sample injected was 2 μL. Phase A of the mobile phase was a water-based solution containing 25 mM ammonium acetate and 25 mM ammonia, whereas Phase B consisted of acetonitrile.

An Orbitrap Exploris 120 mass spectrometer was used because of its capacity to obtain MS/MS spectra through the information-dependent acquisition (IDA) mode, which was regulated using an acquisition software (Xcalibur, Thermo). In this mode, the acquisition software constantly assessed the full-scan MS spectrum. The ESI source parameters were configured as follows: a sheath gas flow rate of 50 Arb, an auxiliary gas flow rate of 15 Arb, a capillary temperature of 320 °C, a full MS resolution of 60000, an MS/MS resolution of 15000, collision energy set at SNCE 20/30/40, and a spray voltage of 3.8 kV (positive) or -3.4 kV (negative).

2.6.3 Data analysis

Metabolome data were imported into the Rapid Identification and Analysis of Metabolic Small Molecules (OSI-SMMS) software to acquire primary and secondary mass spectral data. The data were normalized using the internal standard method, and the parent and fragment ion data were compared against the standard library to derive qualitative results. Principal component analysis (PCA) and orthogonal partial least squares discriminant analysis (OPLS-DA) were performed using the SIMCAV16.0.2 software. Notably, the corresponding OPLS-DA model was constructed 200 times. Additionally, the R and Q values of the stochastic models and the permutation test results were determined. Differentially expressed metabolites between the groups were identified using a *t*-test with the following thresholds: $P < 0.05$ and variable importance in projection (VIP) > 1. Unprocessed data were transformed into the mzXML format using ProteoWizard software, enabling subsequent identification, extraction, alignment, and integration of peak data into a curated secondary mass spectral database via the R package XCMS. Hierarchical clustering analysis was performed using a bioinformatics platform. Visualization and functional elucidation of the metabolomic data were performed using MetaboAnalyst 5.0. Additionally, Kyoto Encyclopedia of Genes and Genomes (KEGG) analysis was performed to determine functions and pathways associated with the metabolites.

2.7 Cell preparation and stimulation

BMDMs were isolated and cultured according to previous reports[21]. After 5 days, the BMDMs were fully differentiated and used for subsequent experiments. To assess inflammasome activity in vitro, BMDMs were seeded in a 12-well tissue culture dish (1.2×10^6 cells/well) and incubated overnight. After stimulating with LPS (500 ng/ml) for 4 h, the cells were treated and incubated with varying concentrations of GR or MCC950 for 1 h, followed by treatment with varying concentrations of PF or 5 mM ATP and further incubation. Finally, the culture supernatants and cell lysates were collected for subsequent analyses.

2.8 Determination of lactate dehydrogenase (LDH) release, MDA, SOD, GSH levels

LDH release were determined using a specific kit (promega, USA), according to the manufacturer's instructions. MDA levels and SOD and GSH activities were determined using the relevant kits according to the manufacturer's instructions.

2.9 ELISA

Serum IL-1β and IL-18 levels were determined using rat IL-1β and IL-18 ELISA kits, respectively.

2.10 Western blotting

Protein extraction from the samples was performed following previously described procedures. Thereafter, proteins were separated on 10% or 12% SDS-PAGE gels and transferred to membranes [29]. After blocking with a blocking buffer for 1 h, the membranes were incubated with the relevant primary antibodies overnight at 4 °C, followed by incubation with secondary antibody at room temperature for 1 h. Finally, the blots were developed using specific reagents.

2.11 Real-time fluorescence quantitative PCR

Rat liver tissue was mixed with Trizol, homogenized, and centrifuged at 12,500 g for 15 min at 4 °C to collect the supernatant. Total RNA was extracted using an RNA extraction kit and reverse-transcribed to generate cDNA using a reverse transcription kit. RT-PCR was performed using 2× RealStar Fast SYBR qPCR Mix, with β-actin as the internal control. The primer sequences are shown below:

β-actin: AGACCTTCAACACCCCAG and CACGATTTCCCTCTCAGC.

IL-1β: TGCTGTCTGACCCATGTGAG and GTCGTTGCTTGTCTCTCCTTG

NLRP3: GTGGAGATCCTAGGTTTCTCTG and CAGGATCTCATTCTCTTGGATC

IL-18: GTGAACCCCAGACCAGACTG and CCTGGAACACGTTTCTGAAAGA

Caspase-1: GAGCTGATGTTGACCTCAGA and CTGTCAGAAGTCTTGTGCTCTG

2.12 Statistical analysis

All statistical analyses were performed using GraphPad 10 software. Significant differences were determined using unpaired Student's *t*-test between two groups and one-way analysis of variance (ANOVA) among multiple groups. Statistical significance was set at $p < 0.05$.

3. Results

3.1 Determination of PF and GR content

Ultra-high performance liquid chromatography (UHPLC) was performed to characterize and identify the major components of PF and GR (Figure 1A and 1B). Notably, PF contained Psoralen, Isopsoralen, Bavachin, Bavachalcone, Psoralidin, Isobavachalcone, Bavachinin, and Bakuchiol at 3.4, 2.77, 0.85, 0.23, 0.18, 0.73, 2.24, and 12.87%, respectively (Table. 1). Additionally, GR contained Liquiritin apioside, Liquiritin, Bavachin, Isoliquiritin, Liquiritigenin, Echinatin, Glycyrrhizic acid, Isoliquiritigenin and Licochalcone A at 1.65, 2.02, 0.44, 0.23, 0.08, 0.10, 5.62, 0.03, and 0.19% respectively (Table. 2).

Table 1 Determination of Psoraleae Fructus

Component	Content (%)	HPLC type	Detection wavelength	Column temperature	Velocity of flow	Standard source
Psoralen	3.40	UItimate XB-C18 4.6*150mm 3μm	246nm	30℃	0.6ml/min	Chengdu pufeide control pin technology co., ltd
Isopsoralen	2.77	UItimate XB-C18 4.6*150mm 3μm	246nm	30℃	0.6ml/min	Chengdu pufeide control pin technology co., ltd
Bavachin	0.85	UItimate XB-C18 4.6*150mm 3μm	246nm	30℃	0.6ml/min	Chengdu pufeide control pin technology co., ltd
Bavachalcone	0.23	UItimate XB-C18 4.6*150mm 3μm	246nm	30℃	0.6ml/min	Chengdu pufeide control pin technology co., ltd
Psoralidin	0.18	UItimate XB-C18 4.6*150mm 3μm	246nm	30℃	0.6ml/min	Chengdu pufeide control pin technology co., ltd
Isobavachalcone	0.73	UItimate XB-C18 4.6*150mm 3μm	246nm	30℃	0.6ml/min	Chengdu pufeide control pin technology co., ltd
Bavachinin	2.24	UItimate XB-C18 4.6*150mm 3μm	246nm	30℃	0.6ml/min	Chengdu pufeide control pin technology co., ltd
Bakuchiol	12.87	UItimate XB-C18 4.6*150mm 3μm	246nm	30℃	0.6ml/min	Chengdu pufeide control pin technology co., ltd

Table 2 Determination of Glycyrrhizae Radix et Rhizoma

Component	Content (%)	HPLC type	Detection wavelength (nm)	Column temperature	Velocity of flow	Standard source
Liquiritin apioside	1.65	UItimate XB-C18 4.6*150mm 3μm	0-50min，236nm；50-56min，375nm	30℃	0.6ml/min	Chengdu pufeide control pin technology co., ltd
Liquiritin	2.02	UItimate XB-C18 4.6*150mm 3μm	0-50min，236nm；50-56min，375nm	30℃	0.6ml/min	Chengdu pufeide control pin technology co., ltd
Isoliquiritin	0.44	UItimate XB-C18 4.6*150mm 3μm	0-50min，236nm；50-56min，375nm	30℃	0.6ml/min	Chengdu pufeide control pin technology co., ltd
Liquiritigenin	0.08	UItimate XB-C18 4.6*150mm 3μm	0-50min，236nm；50-56min，375nm	30℃	0.6ml/min	Chengdu pufeide control pin technology co., ltd
Echinatin	0.10	UItimate XB-C18 4.6*150mm 3μm	0-50min，236nm；50-56min，375nm	30℃	0.6ml/min	Chengdu pufeide control pin technology co., ltd
Glycyrrhizic acid	5.62	UItimate XB-C18 4.6*150mm 3μm	0-50min，236nm；50-56min，375nm	30℃	0.6ml/min	Chengdu pufeide control pin technology co., ltd
Isoliquiritigenin	0.03	UItimate XB-C18 4.6*150mm 3μm	0-50min，236nm；50-56min，375nm	30℃	0.6ml/min	Chengdu pufeide control pin technology co., ltd
Licochalcone A	0.19	UItimate XB-C18 4.6*150mm 3μm	0-50min，236nm；50-56min，375nm	30℃	0.6ml/min	Chengdu pufeide control pin technology co., ltd

A

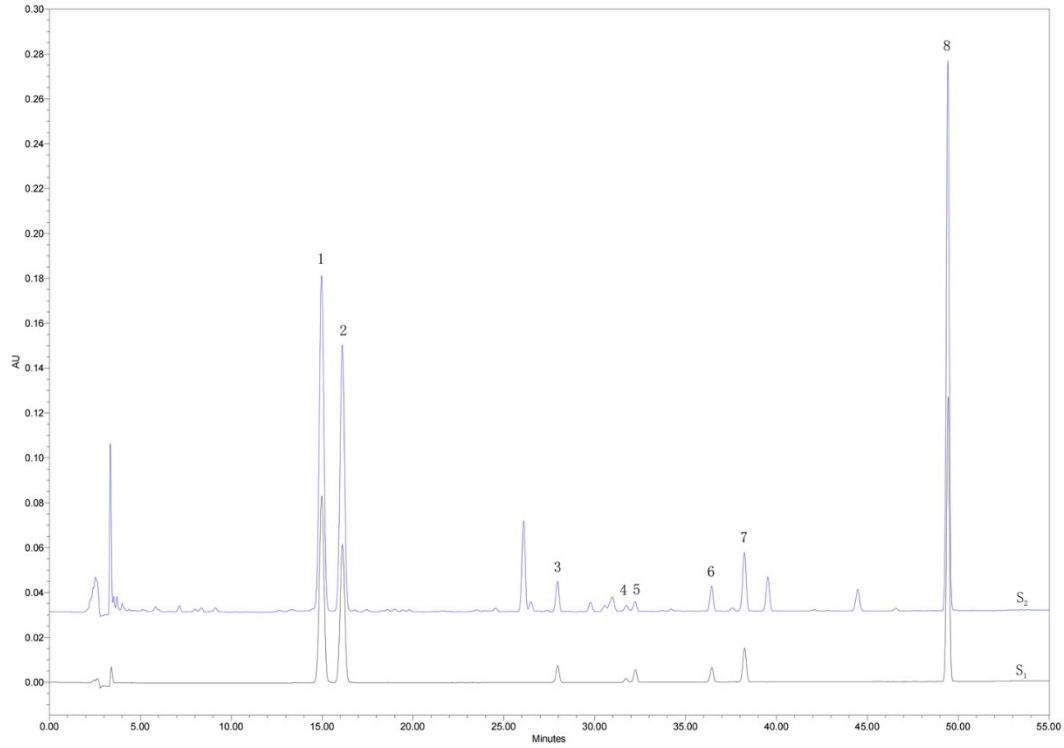

S_1 Mixed control S_2 Psoraleae Fructus

1.Psoralen 2.Isopsoralen 3.Bavachin 4.Bavachalcone 5.Psoralidin 6.Isobavachalcone 7.Bavachinin 8.Bakuchiol

B

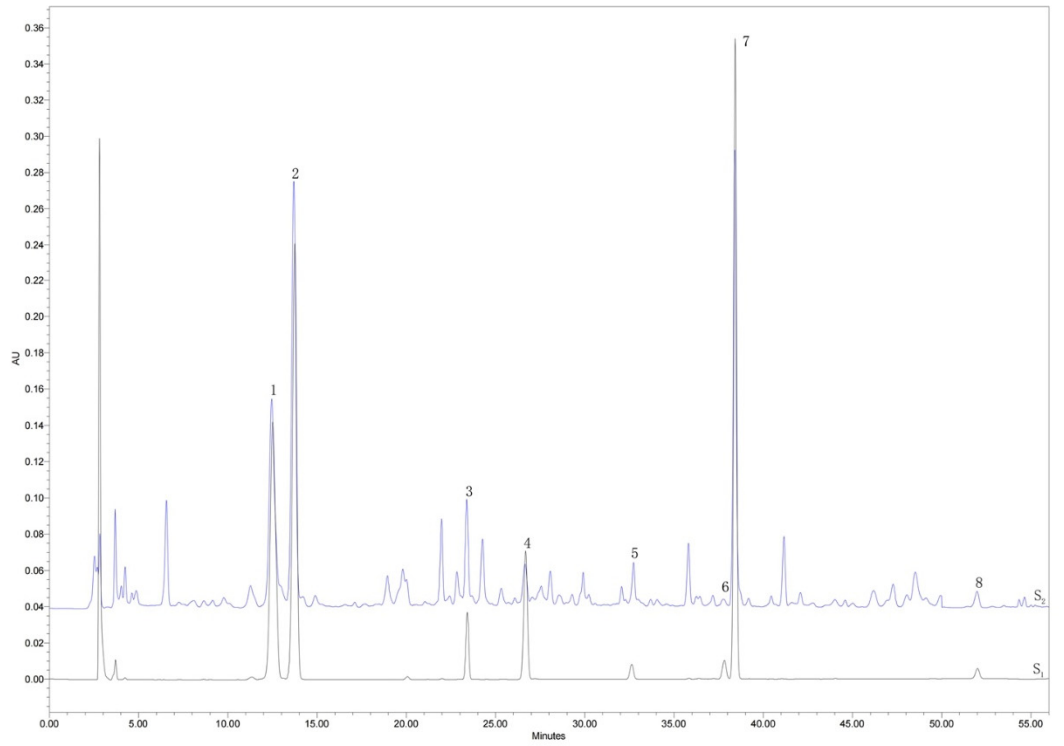

S_1 Mixed control S_2 Glycyrrhizae Radix et Rhizoma

1.Liquiritin apioside 2.Liquiritin 3.Isoliquiritin 4.Liquiritigenin 5.Echinatin 6.Glycyrrhizic acid 7.Isoliquiritigenin 8.Licochalcone A

Figure 1. Levels of major components in PF and GR.

3.2 GR ameliorated PF-induced DILI in rats

To investigate whether GR can mitigate PF-induced liver injury, we established a rat model of immune stress using LPS, a common inducer of DILI. GR (3.6 g/kg) was administered to rats for 3 days via oral gavage. On the final day, GR and PF were co-administered before injecting LPS via the tail vein (Figure 2A). Serum ALT and AST levels were measured to assess liver injury (Figure 2B and C). Notably, there were no significant differences in serum ALT and AST levels between the PF, LPS, and LPS+GR groups, indicating that LPS, PF, and LPS + GR treatment did not induce liver injury in rats under normal conditions. In contrast, serum ALT and AST levels were markedly elevated in the LPS+PF group, indicating that the combination of LPS and PF may induce liver injury in immune-stressed rats. However, GR treatment significantly downregulated the serum levels of these liver injury indicators, suggesting that GR may mitigate PF-induced liver injury. Additionally, we examined the levels of the oxidative stress markers MDA, SOD, and GSH. Importantly, GR treatment alleviated PF-induced increase in MDA levels and reversed PF-induced decrease in SOD and GSH activities (Figure 2D–F). Additionally, we examined the expression of inflammatory factors in the hepatic tissue of the rats using qPCR. Although PF treatment significantly upregulated IL-6 mRNA expression in the hepatic tissue of LPS-stimulated rats, GR administration effectively reduced the inflammatory response (Figure 2G).

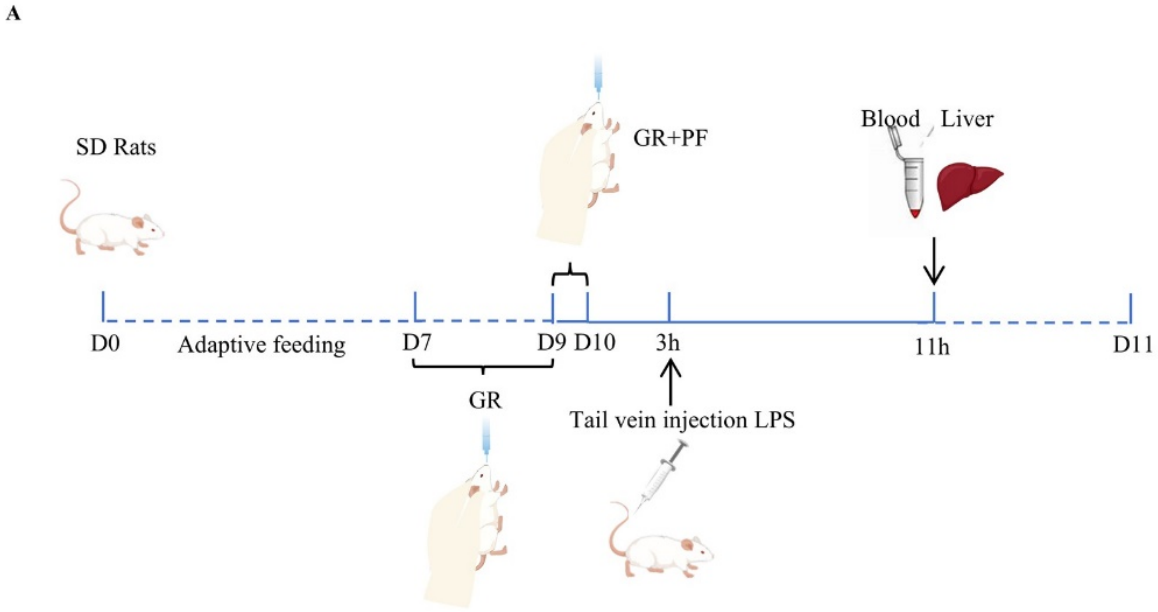

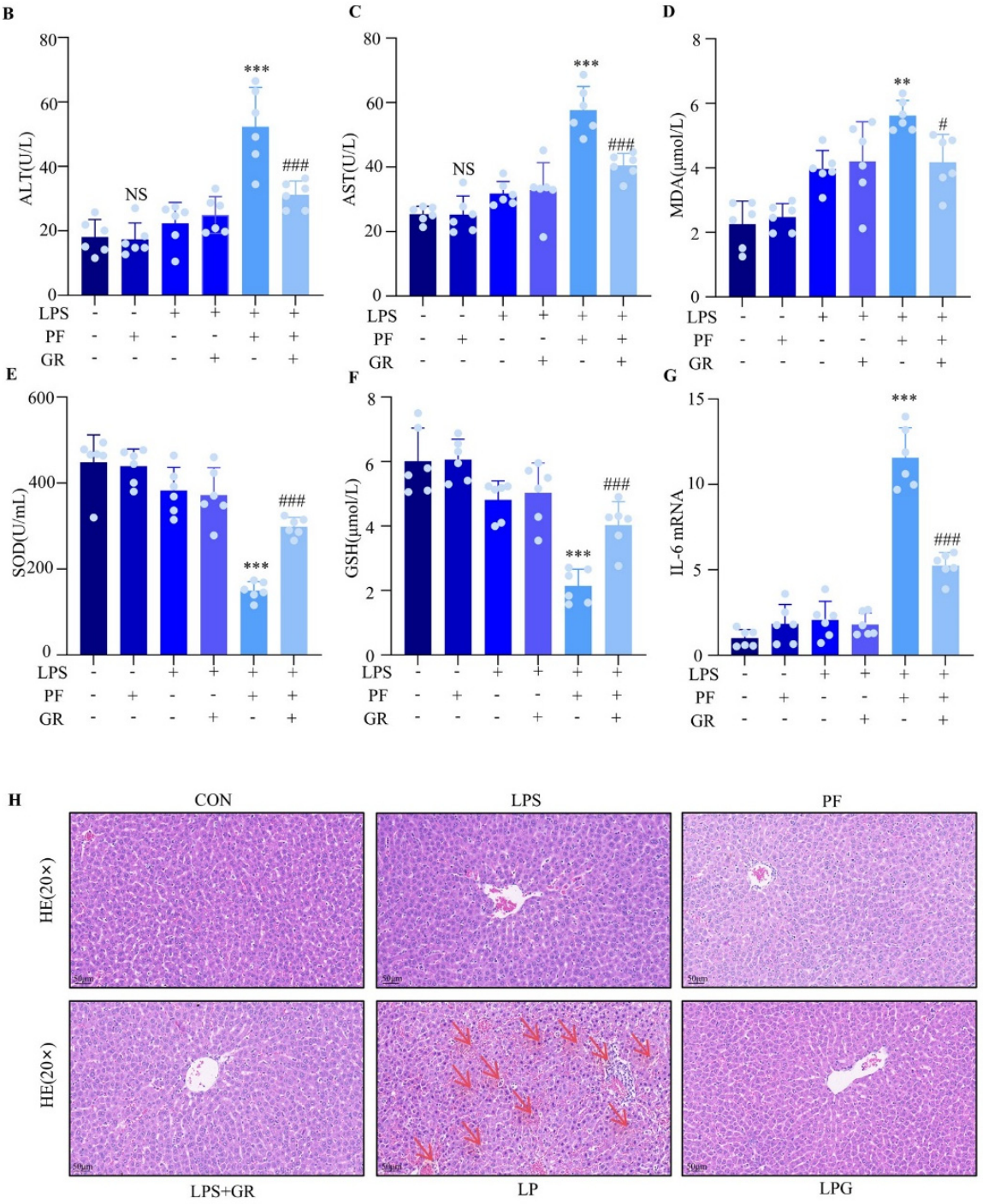

Figure 2. Pretreatment with GR effectively mitigated liver injury caused by PF in rats.

Histological analysis of the liver tissue was performed using H&E staining (Figure 2H). Microscopic examination of liver sections revealed that hepatocyte structure was intact in the control group. Additionally, no significant pathological changes or hepatocyte necrosis were observed in the LPS, PF, and LPS + GR groups. In contrast, hepatocyte steatosis, nuclear aggregation, nuclear fragmentation, and nucleolysis were observed in the LPS+PF group. However, GR treatment significantly reversed these pathological changes in the liver. Collectively, these findings suggest that GR ameliorates PF-induced liver injury.

3.3 GR affects the serum profiles of rats with PF-induced DILI

Considering the crucial role of serum in maintaining metabolic homeostasis, metabolome analysis was performed on serum samples from rats in four groups (CON, LPS, LP, and LPG) to examine metabolic changes. As shown in a PCA score plot, samples in the four groups formed distinct clusters (Figure 3A–B), indicating considerable alterations in the metabolic profiles of the rats. Notably, the scores of the QC samples in the positive and negative ion modes were more clustered in the projection of the score matrix, confirming the stability and reliability of the instrument during the sample onboarding process. Additionally, the OPLS-DA model effectively distinguished between the LP and LPG groups in both the ESI+ and ESI- models (Figure 3C–D). As shown in Figure 3E–F, the scatter plots revealed the distribution of distinct metabolites, indicating changes in the levels of the metabolites among different groups.

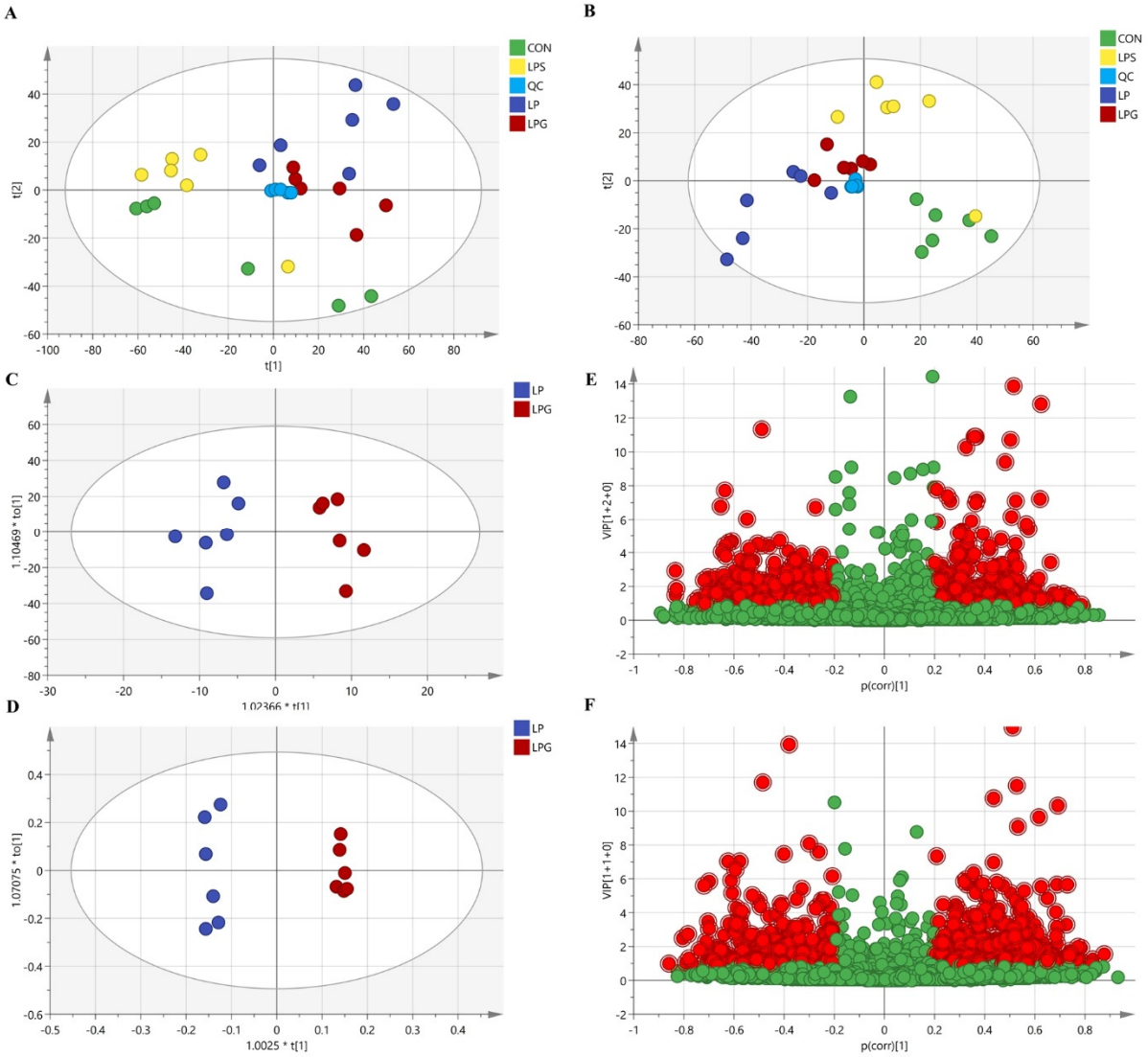

Figure 3. Multivariate statistical analysis results(n = 6).

Radar plots demonstrated that GR significantly reversed the abundance of L-tryptophan, L-glutamate, and L-glutamine (Figure 4A). Additionally, we determined differentially expressed metabolites between the groups based on the VIP (VIP > 1 and $p < 0.05$). Notably, GR treatment significantly downregulated 22 metabolites and significantly upregulated 15 metabolites (Figure 4B). All the differentially expressed metabolites are listed in Supplementary Table 1. Additionally, the metabolic profile of the LPG-treated group

closely resembled that of the LPS group, suggesting that GR significantly mitigated PF-induced DILI. KEGG pathway analysis was performed to determined metabolic pathways associated with the differentially expressed metabolites using MetaboAnalyst 5.0. As illustrated in the bubble plots (Figure 4C), several key metabolic pathways, including pantothenate and CoA biosynthesis, arginine biosynthesis, glycerolipid metabolism, glutamate metabolism, and pyrimidine metabolism were predominantly enriched by metabolites such as glutamine, nervonic acid, fatty acids, histidine, L-tryptophan, N-acetylmannosamine, and L-valine. Collectively, these findings suggest that GR ameliorates PF-induced DILI through multiple metabolic pathways in rats. Accordingly, the biochemical pathways regulated by PF-induced DILI and GR treatment are depicted in Figure 8.

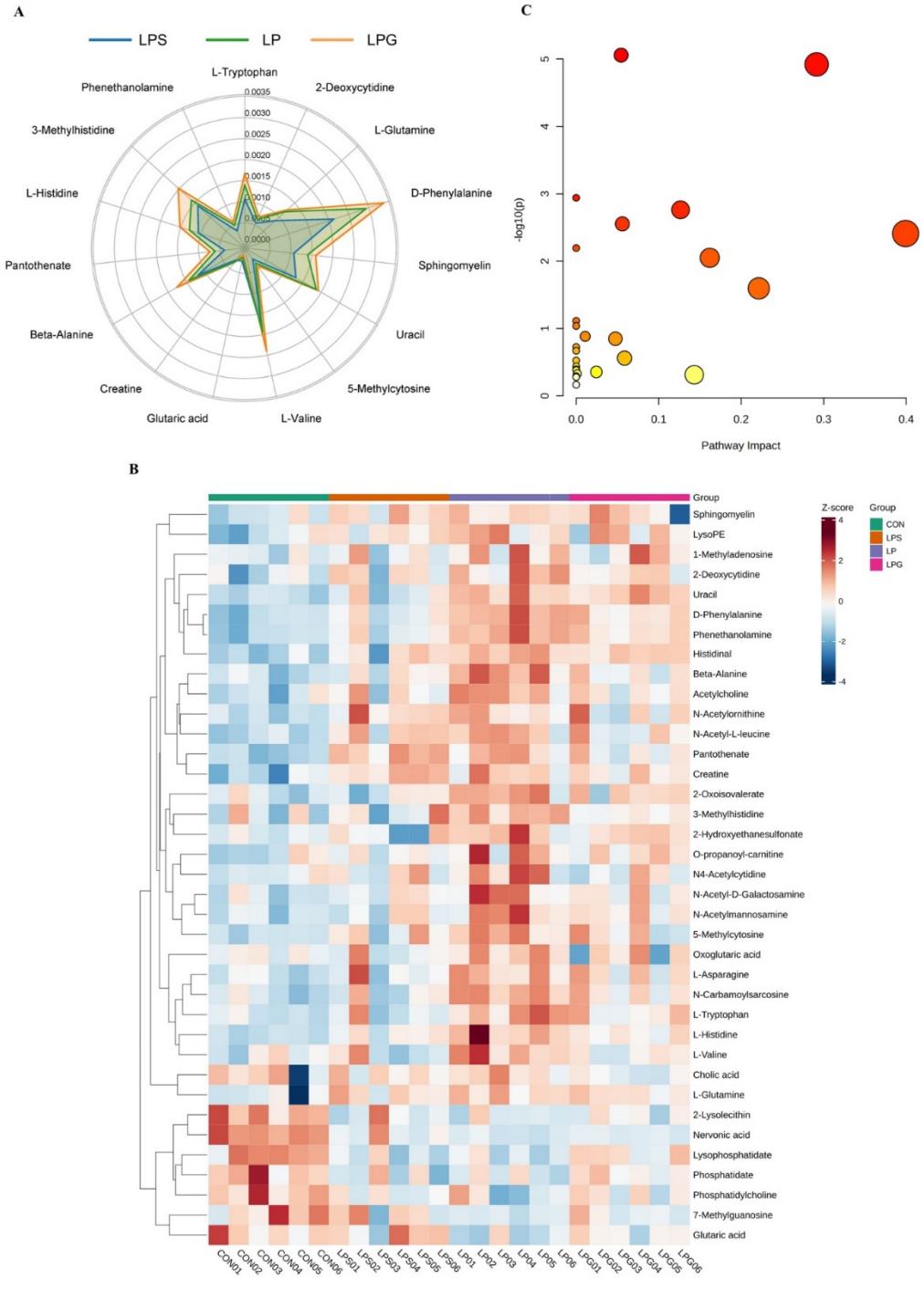

Figure 4. Overall metabolic profile(n = 6).

3.4 PF triggers NLRP3 inflammasome activation

The NLRP3 inflammasome is activated by various external stimuli including Nigericin, ATP, and SiO_2[33, 34]. To determine whether PF-induced DILI is associated with the inflammasome, we exposed BMDMs to LPS for 4 h, followed by the application of MCC950, an NLRP3 inflammasome inhibitor, for 1 h, and PF and ATP for 1 h. As shown in Figure 5A, MCC950 significantly inhibited PF-induced caspase-1 activation and suppressed IL-1β levels, LDH release, and IL-18 levels (Figure 5B–D). Overall, these results confirm that PF directly activates the NLRP3 inflammasome.

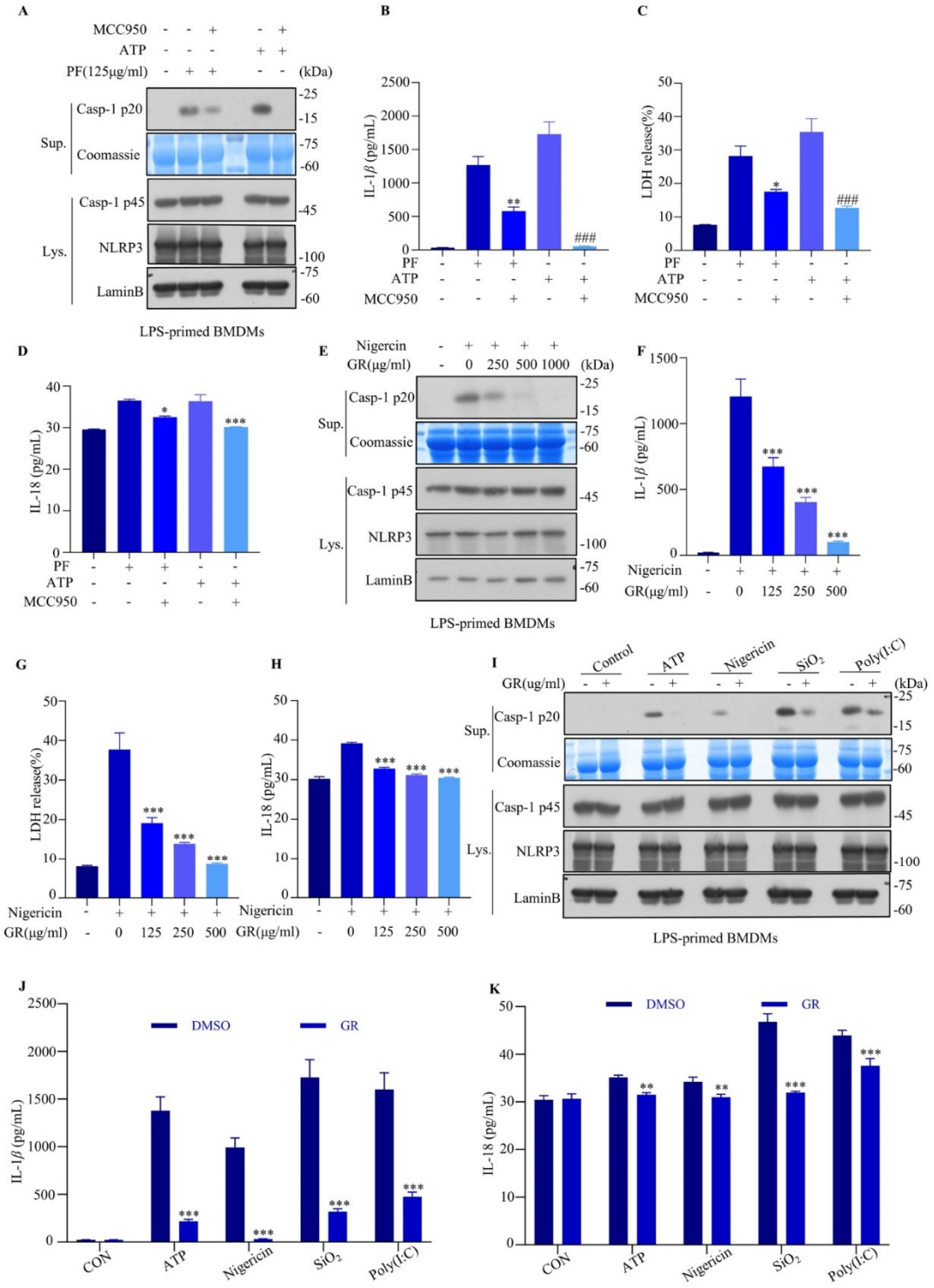

Figure 5. PF promoted NLRP3 inflammasome activation and GR suppressed the activation of the NLRP3 inflammasome in LPS-primed BMDMs.

3.5 GR inhibits NLRP3 inflammasome activation

To investigate the effect of GR-induced NLRP3 inflammasome activation, LPS-pretreated BMDMs were treated with GR treatment for 1 h, and then incubated with nigericin for 1 h. GR effectively inhibited ATP-induced activation of NLRP3 inflammasome in a dose-dependent manner (Figure 5E–H), leading to a progressive decrease in caspase-1 maturation, IL-1β and IL-18 secretion, and LDH release. Additionally, we examined whether GR can inhibit NLRP3 inflammasome activation induced by various NLRP3 inflammasome agonists, including nigericin, SiO_2, and poly(I:C). GR effectively inhibited caspase-1 maturation and suppressed the agonist-induced increase in IL-1β and IL-18 levels (Figure 5I–K).

3.6 GR inhibits PF-induced NLRP3 inflammasome activation

To confirm the effect of GR on PF-induced inflammation, we investigated whether GR inhibits PF-induced activation of the NLRP3 inflammasome. LPS-primed BMDMs were incubated with GR for 1 h, followed by PF for 1 h (Figure 6A–D). Although PF treatment alone induced caspase-1 (p20) maturation and increased IL-1β, LDH, and IL-18 levels, GR co-treated treatment reversed these effects. Overall, these results indicate that GR may inhibit PF-induced activation of the NLRP3 inflammasome. Echinatin, a constituent of the GR, has been shown to inhibit NLRP3 inflammasome activation. Therefore, we investigated whether Echinatin inhibits PF-induced NLRP3 inflammasome activation. Cells incubated with Echinatin for 1 h were treated with PF (Figure 6E–J). Echinatin pretreatment inhibited PF-induced caspase-1 p20 expression and downregulated LDH release, IL-1β, and IL-18 levels. Overall, these results provide additional evidence that GR suppresses PF-induced inflammasome activation.

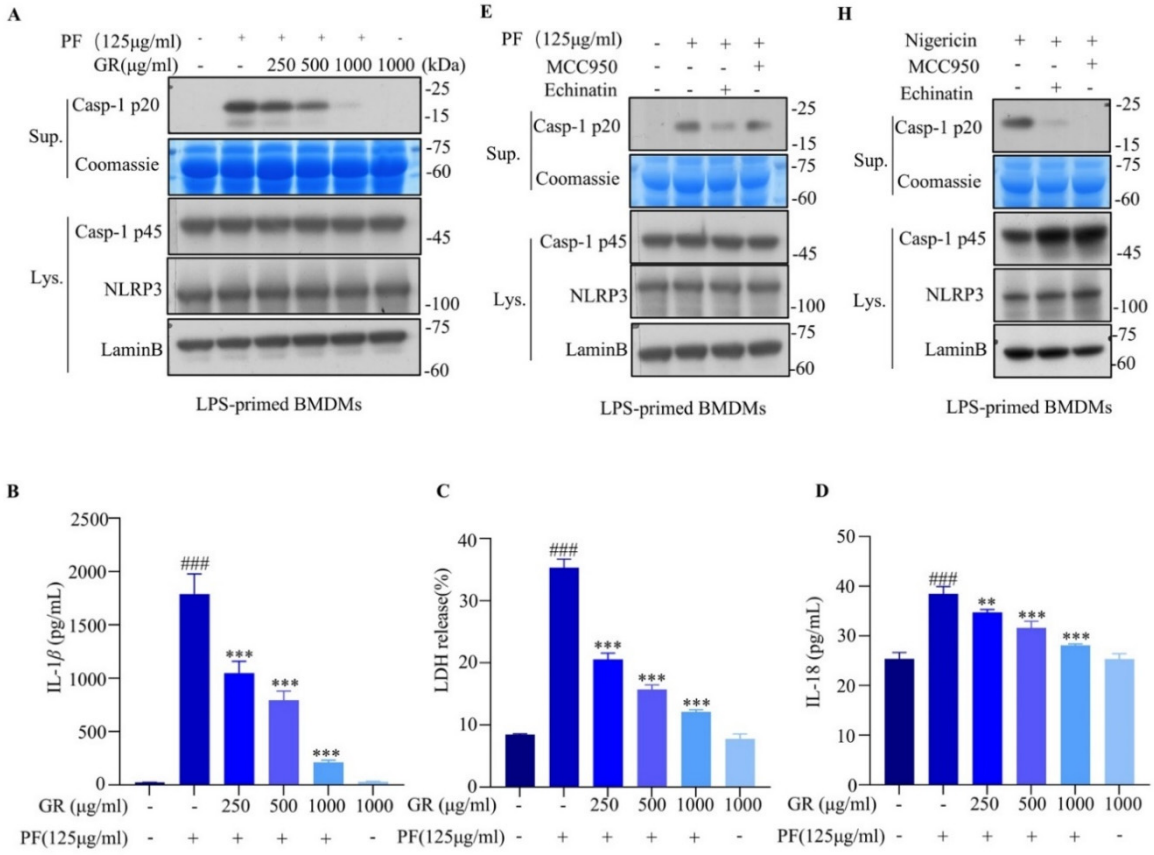

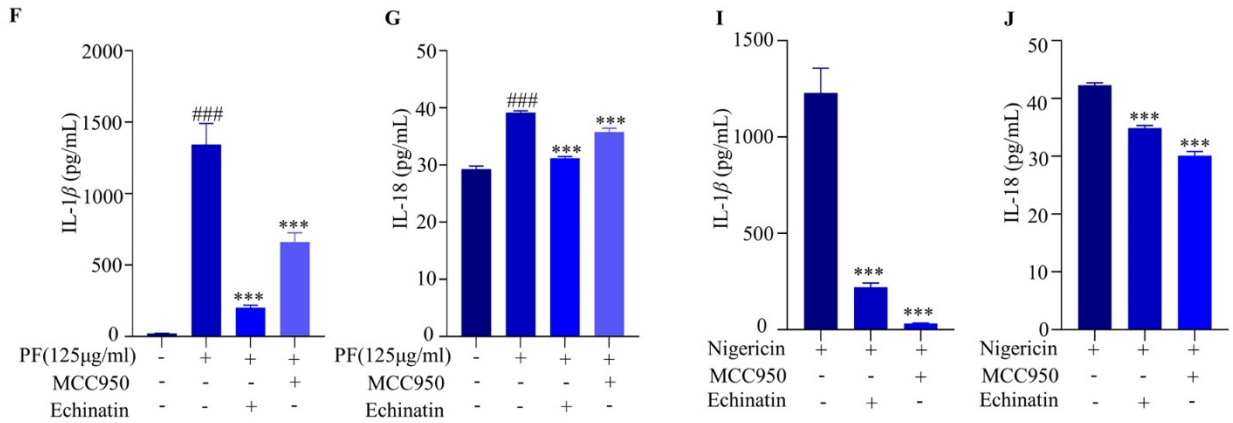

Figure 6. GR blocked PF-induced inflammasome activation.

To further verify that GR attenuates PF-induced liver injury via inhibition of NLRP3 inflammasome, we examined the serum levels of IL-1β and IL-18. IL-1β concentration was significantly higher in the LPS+PF group compared to the LPS group. In contrast, IL-1β levels were significantly lower in the LPS+PF+GR group than in the LPS+PF group, and a similar trend was observed for IL-8 (Figure 7A–B). Additionally, we examine the mRNA levels of IL-1β, IL-18, NLRP3, and caspase-1 in rat liver tissue. Although IL-1β, IL-18, NLRP3, and caspase-1 mRNA expression was significantly upregulated in the LPS+PF group compared with those in the control group, GR treatment significantly downregulated the inflammatory factors (Figure 7C–F). Overall, these results indicate that GR ameliorates LPS- and PF-induced liver injury via inhibition of NLRP3 inflammasome, which was consistent with the results of the metabolomic analysis.

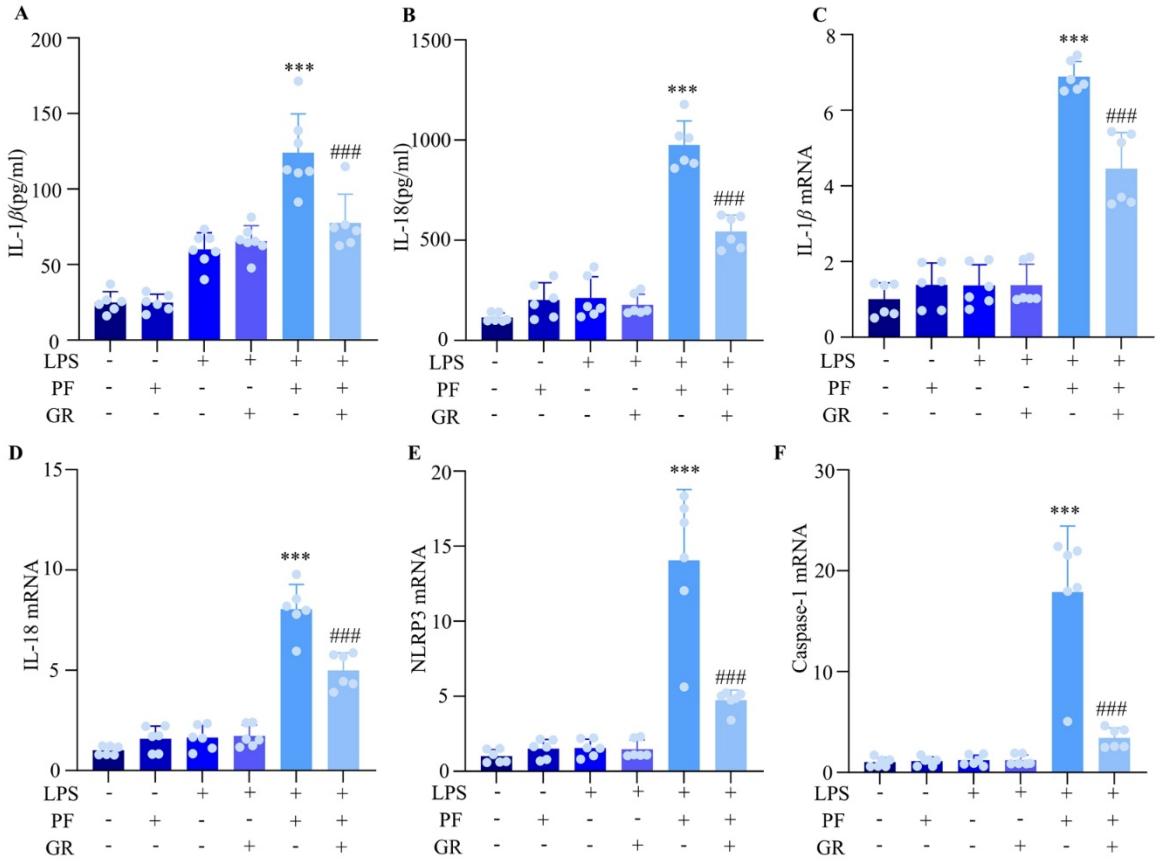

Figure 7. GR ameliorates PF-induced DILI and modulates NLRP3 inflammasome.

4. Discussion

DILI accounts for a significant proportion of non-viral liver diseases and is highly prevalent, representing a major cause of preclinical and clinical drug termination [35, 36]. Recently, PF-induced liver injury has raised considerable concerns[37]. Research findings indicate that ALT and AST are common indicators of liver pathologies. Long-term oxidative stress, coupled with hepatic inflammatory responses, are defining characteristics of DILI [38]. Our study showed that the medicinal herb GR effectively mitigated PF-induced DILI in a rat model of immune stress. Additionally, rats in the LPS and PF groups showed a marked increase in the serum levels of the hepatic damage indicators ALT and AST. Moreover, LPS and PF treatment markedly upregulated the levels of the inflammatory cytokines IL-6 and MDA and significantly downregulated SOD and GSH activities. Notably, GR co-treatment effectively reversed PF-induced alterations in the levels of these indicators, suggesting that GR mitigated PF-induced liver injury.

Metabolic disorders represent significant pathophysiological alterations in the pathogenesis of liver injury[39, 40]. Metabolomic analysis provides insight on complex pathophysiological processes of DILI [41]. In this study, metabolomic analysis of rats serum samples from the four groups revealed significant differences in the metabolite profiles before and after drug administration. Among the identified metabolites, 37 were significantly modulated following GR treatment. KEGG analysis showed that glutamine, nervonic acid, fatty acid, histidine, L-tryptophan, N-acetylmannosamine, and L-valine were significantly enriched in the following metabolic pathways: arginine biosynthesis; glycerolipid, pyrimidine, beta-alanine, and pantothenate metabolism; CoA biosynthesis; and alanine, aspartate, and glutamate metabolism pathways. Importantly, these pathways and metabolites may be central to the mechanism by which GR ameliorates PF-induced DILI. Glutaminase inhibition suppresses the anaerobic conversion of glutamine to the tricarboxylic acid cycle and amino acid synthesis, promotes mitochondrial autophagy, and inhibits the accumulation of intracellular reactive oxygen species (ROS), ultimately preventing the activation of NLRP3 inflammasomes in microglial cells during Alzheimer's disease[42]. Fatty acids ameliorate NASH by promoting the release of mitochondrial DNA, which induces the release of ROS, thereby activating the NLRP3 inflammasome in mouse Kupffer cells[43]. Danyu Tongwei granules significantly reduced valine, leucine, and isoleucine synthesis, thereby inhibiting myocardial infarction by suppressing isoproterenol-induced NLRP3 inflammasome activation in rats[43]. Collectively, these findings suggest that the metabolites and NLRP3 inflammasome activation are inextricably linked. Therefore, we hypothesized that GR-mediated amelioration of PF-induced DILI is associated with NLRP3 inflammasome.

Inflammasome activation triggers an inflammatory response closely linked to DILI[44]. In this study, we established an LPS-induced NLRP3 inflammasome model to elucidate the mechanism by which GR attenuates PF-induced hepatotoxicity. PF directly induced NLRP3 inflammasome activation, resulting in caspase-1 activation and increased IL-1β, IL-18 levels, and LDH release. However, GR treatment effectively inhibited NLRP3 inflammasome activation in a dose-dependent manner. GR and PF co-treatment significantly inhibited PF-induced inflammasome and caspase-1 activation and inhibited PF-induced increase

in IL-1β and IL-18 levels. Mechanistically, GR attenuated PF-induced DILI by inhibiting inflammasome activation. Additionally, Echinatin, the active component of GR, exhibited a similar inhibitory effect on PF-induced NLRP3 inflammasome activation. Our study provide additional evidence to support the use of GR for the treatment of PF-induced DILI.

In a rat model, we observed that GR treatment significantly attenuated LPS + PF-induced increased in serum IL-1β and IL-18 levels. However, GR treatment significantly inhibited PF-induced upregulation of the mRNA expression of key components of the NLRP3 inflammasome pathway (IL-1β, IL-18, NLRP3, and caspase-1) in the liver tissue of the rats. Collectively, these findings confirm that GR alleviates PF-induced liver injury by inhibiting NLRP3 inflammasome activation, indicating the potential of GR in ameliorating PF-induced DILI.

Previous studies have shown that GR exhibits diverse therapeutic effects, including antitumor, anti-inflammatory, antibacterial, antiviral, neuroprotective, and hepatoprotective properties[16]. Notably, GR has the unique ability to act as a flavor enhancer, similar to candy and beverage additives[45]. As an effective measure to prevent potential PF-induced hepatotoxicity, the consumption of foods containing GR before ingesting PF-containing drugs is recommended. However, PF and GR co-administration should be considered on a case-by-case basis. Although some studies have suggested that the inflammasome pathway plays a protective role in tumorigenesis, the expression of all NLRP3 inflammasome components are either absent or markedly reduced in human hepatocellular carcinoma. This deficiency is strongly associated with an advanced disease stage and poor pathological differentiation[46]. Therefore, when PF is used as an anti-HCC, it may not be necessary to co-administer GR.

Despite the promising findings, this study has several limitations. Additional experiments, including immunofluorescence and immunohistochemistry, are necessary to confirm whether GR ameliorates DILI by inhibiting PF-induced NLRP3 inflammasome activation. Additionally, the ability of GR to ameliorate PF hepatotoxicity has only been demonstrated in rat models, both in vivo and in vitro, with no corresponding clinical evidence.

Future studies should aim to conduct comprehensive preclinical toxicity evaluations and dose optimization experiments to better understand the safety profile of GR and PF co-administration. Considering that our current findings were based solely on rat models, it is crucial to recognize the potential differences in drug metabolism and immune responses between animals and humans. These interspecies differences could significantly influence both the efficacy and safety of GR, as human liver enzyme systems and immune regulation often differ from those of rodents. Therefore, translational studies using human liver organoids or humanized animal models may provide clinically relevant insights. Furthermore, well-designed clinical trials are essential to validate the hepatoprotective effects of GR in human populations, determine optimal dosing strategies, and assess potential herb-drug interactions in patients receiving PF therapy. Exploring these avenues will not only enhance the translational potential of our findings but facilitate the clinical application of GR in the prevention and treatment of PF-induced DILI.

5. Conclusion

In this study, we elucidated the potential mechanism by which GR prevents and treats PF-induced DILI. Our findings indicate that GR significantly mitigates PF-induced liver injury by inhibiting PF-induced NLRP3 inflammasome activation (Fig. 8). Conclusively, this study offers a novel therapeutic strategy for managing PF-induced hepatotoxicity, providing a scientific foundation for reducing the safety risks of potentially toxic Chinese medicinal herbs.

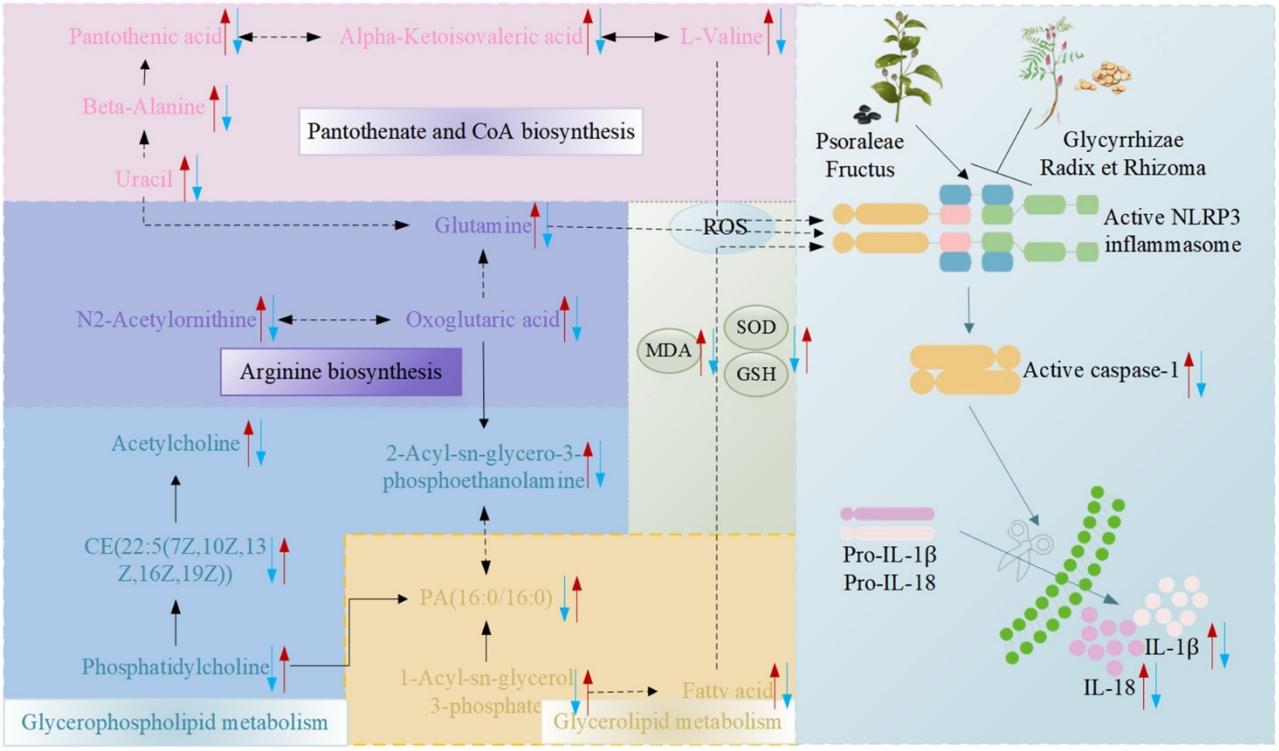

Figure 8. GR ameliorated DILI caused by PF and modulated the NLRP3 inflammasome metabolic network.

Conflicts of Interest

The authors declare no conflicts of interest.

Acknowledgments

This work was supported by the project of National Natural Science Foundation of China (U23A20519, 82230118, 82474095, 82204638), the project of State Administration of Traditional Chinese Medicine High-level Chinese Medicine Key Discipline Construction Project (zyyzdxk-2023309).

References

[1] A.I. Shehu, X. Ma, R. Venkataramanan, Mechanisms of Drug-Induced Hepatotoxicity, Clin Liver Dis. 21 (2017) 35-54. https://doi.org/10.1016/j.cld.2016.08.002.

[2] R.J. Fontana, E.S. Bjornsson, R. Reddy, et al., The Evolving Profile of Idiosyncratic Drug-Induced Liver Injury, Clin Gastroenterol Hepatol. 21 (2023) 2088-2099. https://doi.org/10.1016/j.cgh.2022.12.040.

[3] Z.T. Ma, Z. Shi, X.H. Xiao, et al., New Insights into Herb-Induced Liver Injury, Antioxid Redox Signal. 38 (2023) 1138-1149. https://doi.org/10.1089/ars.2022.0134.

[4] S.W. Nam, J.T. Baek, D.S. Lee, et al., A case of acute cholestatic hepatitis associated with the seeds of Psoralea corylifolia (Boh-Gol-Zhee), Clin Toxicol (Phila). 43 (2005) 589-591. https://doi.org/10.1081/clt-200068863.

[5] H.J. Gandhi, S. Chandnani, A. Jena, et al., A Rare Cause of Acute on Chronic Liver Failure (ACLF): Bakuchi-Induced Liver Injury, J Clin Exp Hepatol. 14 (2024) 101267. https://doi.org/10.1016/j.jceh.2023.08.003.

[6] L. Chen, S. Chen, P. Sun, et al., Psoralea corylifolia L.: a comprehensive review of its botany, traditional uses, phytochemistry, pharmacology, toxicology, quality control and pharmacokinetics, Chin Med. 18 (2023) 4. https://doi.org/10.1186/s13020-022-00704-6.

[7] Y. Xu, X. Wang, Y. Wang, et al., New compatible pair of TCM: Paeoniae Radix Alba effectively alleviate Psoraleae Fructus-induced liver injury by suppressing NLRP3 inflammasome activation, Heliyon. 10 (2024) e34591. https://doi.org/10.1016/j.heliyon.2024.e34591.

[8] B. Liu, S. Fang, K. Zhou, et al., Unveiling hepatotoxicity distinction of coumarin-related compounds from glycosides to aglycones in Fructus Psoraleae by integrating UPLC-Q-TOF-MS and high content analysis, J Ethnopharmacol. 315 (2023) 116664. https://doi.org/10.1016/j.jep.2023.116664.

[9] Y. Yang, X. Tang, F. Hao, et al., Bavachin Induces Apoptosis through Mitochondrial Regulated ER Stress Pathway in HepG2 Cells, Biol Pharm Bull. 41 (2018) 198-207. https://doi.org/10.1248/bpb.b17-00672.

[10] Y. Wang, G. Xu, Z. Wang, et al., Psoralidin, a major component of Psoraleae Fructus, induces inflammasome activation and idiosyncratic liver injury, Int Immunopharmacol. 92 (2021) 107352. https://doi.org/10.1016/j.intimp.2020.107352.

[11] T. Liu, G. Xu, Y. Li, et al., Discovery of bakuchiol as an AIM2 inflammasome activator and cause of hepatotoxicity, J Ethnopharmacol. 298 (2022) 115593. https://doi.org/10.1016/j.jep.2022.115593.

[12] W. Shi, Y. Gao, H. Yang, et al., Bavachinin, a main compound of Psoraleae Fructus, facilitates GSDMD-mediated pyroptosis and causes hepatotoxicity in mice, Chem Biol Interact. 400 (2024) 111133. https://doi.org/10.1016/j.cbi.2024.111133.

[13] Y. Ding, E. Brand, W. Wang, et al., Licorice: Resources, applications in ancient and modern times, J Ethnopharmacol. 298 (2022) 115594. https://doi.org/10.1016/j.jep.2022.115594.

[14] S. Wahab, S. Annadurai, S.S. Abullais, et al., Glycyrrhiza glabra (Licorice): A Comprehensive Review on Its Phytochemistry, Biological Activities, Clinical Evidence and Toxicology, Plants (Basel). 10 (2021) https://doi.org/10.3390/plants10122751.

[15] H. Zhang, H. Ouyang, J. Zhang, et al., Exploring the efficacy and mechanism of Glycyrrhizae Radix et Rhizoma in improving collagen-induced arthritis in mice, J Ethnopharmacol. 322 (2024) 117554. https://doi.org/10.1016/j.jep.2023.117554.

[16] Y. Zhang, J. Lu, T. Chang, et al., A bibliometric review of Glycyrrhizae Radix et Rhizoma (licorice) research: Insights and future directions, J Ethnopharmacol. 321 (2024) 117409. https://doi.org/10.1016/j.jep.2023.117409.

[17] X. Duan, J. Wen, M. Zhang, et al., Glycyrrhiza uralensis Fisch. and its active components mitigate Semen Strychni-induced neurotoxicity through regulating high mobility group box 1 (HMGB1) translocation, Biomed Pharmacother. 149 (2022) 112884. https://doi.org/10.1016/j.biopha.2022.112884.

[18] H.Z. Li, B. Liu, H.Y. Shu, et al., [Toxicity-reducing effect of compatibility of Tripterygium and licorice in animals: systematic review], Zhongguo Zhong Yao Za Zhi. 44 (2019) 3512-3519. https://doi.org/10.19540/j.cnki.cjcmm.20181214.002.

[19] W. Luo, G. Xu, Z. Song, et al., Licorice extract inhibits the cGAS-STING pathway and protects against non-alcoholic steatohepatitis, Front Pharmacol. 14 (2023) 1160445. https://doi.org/10.3389/fphar.2023.1160445.

[20] Q. Li, H. Feng, H. Wang, et al., Licochalcone B specifically inhibits the NLRP3 inflammasome by disrupting NEK7-NLRP3 interaction, EMBO Rep. 23 (2022) e53499. https://doi.org/10.15252/embr.202153499.

[21] G. Xu, S. Fu, X. Zhan, et al., Echinatin effectively protects against NLRP3 inflammasome-driven diseases by targeting HSP90, JCI Insight. 6 (2021) https://doi.org/10.1172/jci.insight.134601.

[22] Y. Liu, W. Guo, M. Li, Diammonium Glycyrrhizinate Preparation for Liver Function Recovery in Chronic Hepatitis B in China: A Meta-analysis with Trial Sequential Analysis, Curr Pharm Des. 28 (2022) 2089-2112. https://doi.org/10.2174/1381612828666220421134910.

[23] D. Zheng, T. Liwinski, E. Elinav, Inflammasome activation and regulation: toward a better understanding of complex mechanisms, Cell Discov. 6 (2020) 36. https://doi.org/10.1038/s41421-020-0167-x.

[24] Y. Ga, Y. Wei, Q. Zhao, et al., Puerariae Radix protects against ulcerative colitis in mice by inhibiting NLRP3 inflammasome activation, Food Sci Hum Wellness. 13 (2024) 2266-2276. https://doi.org/10.26599/FSHW.2022.9250189.

[25] J. Yao, K. Sterling, Z. Wang, et al., The role of inflammasomes in human diseases and their potential as therapeutic targets, Signal Transduct Target Ther. 9 (2024) 10. https://doi.org/10.1038/s41392-023-01687-y.

[26] H. Guo, J.B. Callaway, J.P. Ting, Inflammasomes: mechanism of action, role in disease, and therapeutics, Nat Med. 21 (2015) 677-687. https://doi.org/10.1038/nm.3893.

[27] K. Fujimura, T. Karasawa, T. Komada, et al., NLRP3 inflammasome-driven IL-1β and IL-18 contribute to lipopolysaccharide-induced septic cardiomyopathy, J Mol Cell Cardiol. 180 (2023) 58-68. https://doi.org/10.1016/j.yjmcc.2023.05.003.

[28] Q. Ma, Pharmacological Inhibition of the NLRP3 Inflammasome: Structure, Molecular Activation, and Inhibitor-NLRP3 Interaction, Pharmacol Rev. 75 (2023) 487-520. https://doi.org/10.1124/pharmrev.122.000629.

[29] H. Liu, X. Zhan, G. Xu, et al., Cryptotanshinone specifically suppresses NLRP3 inflammasome activation and protects against inflammasome-mediated diseases, Pharmacol Res. 164 (2021) 105384. https://doi.org/10.1016/j.phrs.2020.105384.

[30] Z. Wang, G. Xu, Y. Gao, et al., Cardamonin from a medicinal herb protects against LPS-induced septic shock by suppressing NLRP3 inflammasome, Acta Pharm Sin B. 9 (2019) 734-744. https://doi.org/10.1016/j.apsb.2019.02.003.

[31] J. Zhao, H. Liu, Z. Hong, et al., Tanshinone I specifically suppresses NLRP3 inflammasome activation by disrupting the association of NLRP3 and ASC, Mol Med. 29 (2023) 84. https://doi.org/10.1186/s10020-023-00671-0.

[32] W. Shi, G. Xu, X. Zhan, et al., Carnosol inhibits inflammasome activation by directly targeting HSP90 to treat inflammasome-mediated diseases, Cell Death Dis. 11 (2020) 252. https://doi.org/10.1038/s41419-020-2460-x.

[33] S. Paik, J.K. Kim, P. Silwal, et al., An update on the regulatory mechanisms of NLRP3 inflammasome activation, Cell Mol Immunol. 18 (2021) 1141-1160. https://doi.org/10.1038/s41423-021-00670-3.

[34] E.K. Jo, J.K. Kim, D.M. Shin, et al., Molecular mechanisms regulating NLRP3 inflammasome activation, Cell Mol Immunol. 13 (2016) 148-159. https://doi.org/10.1038/cmi.2015.95.

[35] T. Yokoi, S. Oda, Models of Idiosyncratic Drug-Induced Liver Injury, Annu Rev Pharmacol Toxicol. 61 (2021) 247-268. https://doi.org/10.1146/annurev-pharmtox-030220-015007.

[36] K.T. Suk, D.J. Kim, Drug-induced liver injury: present and future, Clin Mol Hepatol. 18 (2012) 249-257. https://doi.org/10.3350/cmh.2012.18.3.249.

[37] F.L. Ge, M. Niu, Z.X. Han, et al., Landscape of Hepatobiliary Adverse Drug Reactions Related to Preparations Containing Psoraleae Fructus and Its Application in Pharmacovigilance, Chin J Integr Med. 27 (2021) 832-837. https://doi.org/10.1007/s11655-021-3442-2.

[38] W.R. Kim, S.L. Flamm, A.M. Di Bisceglie, et al., Serum activity of alanine aminotransferase (ALT) as an indicator of health and disease, Hepatology. 47 (2008) 1363-1370. https://doi.org/10.1002/hep.22109.

[39] J.T. Qiao, C. Cui, L. Qing, et al., Activation of the STING-IRF3 pathway promotes hepatocyte inflammation, apoptosis and induces metabolic disorders in nonalcoholic fatty liver disease, Metabolism. 81 (2018) 13-24. https://doi.org/10.1016/j.metabol.2017.09.010.

[40] Y. Shu, D. He, W. Li, et al., Hepatoprotective Effect of Citrus aurantium L. Against APAP-induced Liver Injury by Regulating Liver Lipid Metabolism and Apoptosis, Int J Biol Sci. 16 (2020) 752-765. https://doi.org/10.7150/ijbs.40612.

[41] J. Yang, M. Zhang, Y. Luo, et al., Protopine ameliorates OVA-induced asthma through modulatingTLR4/MyD88/NF-κB pathway and NLRP3 inflammasome-mediated pyroptosis, Phytomedicine. 126 (2024) 155410. https://doi.org/10.1016/j.phymed.2024.155410.

[42] Z. Zhang, M. Li, X. Li, et al., Glutamine metabolism modulates microglial NLRP3 inflammasome activity through mitophagy in Alzheimer's disease, J Neuroinflammation. 21 (2024) 261. https://doi.org/10.1186/s12974-024-03254-w.

[43] J. Pan, Z. Ou, C. Cai, et al., Fatty acid activates NLRP3 inflammasomes in mouse Kupffer cells through mitochondrial DNA release, Cell Immunol. 332 (2018) 111-120. https://doi.org/10.1016/j.cellimm.2018.08.006.

[44] L. Shi, S. Zhang, Z. Huang, et al., Baicalin promotes liver regeneration after acetaminophen-induced liver injury by inducing NLRP3 inflammasome activation, Free Radic Biol Med. 160 (2020) 163-177. https://doi.org/10.1016/j.freeradbiomed.2020.05.012.

[45] H. Seki, K. Ohyama, S. Sawai, et al., Licorice beta-amyrin 11-oxidase, a cytochrome P450 with a key role in the biosynthesis of the triterpene sweetener glycyrrhizin, Proc Natl Acad Sci U S A. 105 (2008) 14204-14209. https://doi.org/10.1073/pnas.0803876105.

[46] H. Zhao, Y. Zhang, Y. Zhang, et al., The role of NLRP3 inflammasome in hepatocellular carcinoma, Front Pharmacol. 14 (2023) 1150325. https://doi.org/10.3389/fphar.2023.1150325.